TREND-SIGNAL MODELLING OF LAND SUBSIDENCE

Frank Kenselaar[1] and Raoul Quadvlieg[2]

[1]*Delft University of Technology, Department of Mathematical Geodesy and Positioning, Thijsseweg 11, 2629 JA Delft, The Netherlands (f.kenselaar@geo.tudelft.nl)*

[2]*Nederlandse Aardolie Maatschappij B.V., Geomatics Department, P.O. Box 28000 9400 HH Assen, The Netherlands (r.c.h.quadvlieg@nam.nl)*

Abstract

In this paper a new approach will be discussed for describing land subsidence due to the extraction of hydrocarbons. In order to exploit the smooth and gradual subsidence behavior above deep gas reservoirs, a rather simple parametric spatial-temporal trend model is employed as an approximation of the subsidence bowl at the centimeter level. An optimal fit of the trend model is obtained through an estimation procedure using extensive hypothesis testing. The model is determined from the original multi-epoch levelling data, avoiding the cumbersome connection to stable reference points. Special attention is paid to the stochastic model, distinguishing levelling measurement noise, stochastic benchmark instability and model imperfections.
The least-squares residuals to the levelling data include, amongst measurement noise and individual benchmark instability, the remaining subsidence due to gas extraction, which is not described by the trend approximation. Computation and visualization of this signal could reveal spatial and/or temporal coherent deviations from the trend, that require further analysis in order to facilitate a detailed match with production history. The approach is demonstrated on two cases: a subsidence area above an isolated gas and oil field, and a more complex area with overlapping subsidence bowls above several gas fields.

1. Introduction

Since 1964 gas is extracted from the large Groningen gas field and its smaller adjacent fields, in the northeast of The Netherlands. Although the resulting land subsidence has a smooth character and does not exceed the few decimeter level, the subsidence is monitored extensively because the subsiding area is largely situated below sea level and requires careful water management. Different aspects of the Groningen subsidence have been described in BARENDS ET AL. 1995.
Although also other measurement types have been used, like GPS and InSAR, the main data source for subsidence monitoring are the levelling networks that have been surveyed every 1-5 years. In order to support the subsidence analysis, a processing strategy has been developed, consisting of three steps (DE HEUS ET AL. 1995): 1) Single epoch analysis of the levelling networks; 2) Stability analysis of the levelling benchmarks and connection of the levelling networks to stable reference points (DE HEUS ET AL. 1994); 3) Kinematic deformation analysis based on estimation of a polynomial subsidence curve per benchmark (VERHOEF AND DE HEUS 1995). In each step the estimation of an optimal model was supported by an extensive testing procedure for detection of data errors and suggestion of model adaptations.

Although this procedure worked quite well, certain drawbacks were experienced. Absolute deformation analysis, by connection of the levelling networks to stable benchmarks, was complicated by the expanding subsidence area and the suspicion of unstable reference points. Stability analysis, in order to identify stable reference points, turned out to be the most difficult part of the data processing. Moreover, the benchmark-oriented analysis was frustrated because many benchmarks disappeared during the years, and new benchmarks in larger levelling networks had to be established to cover the growing subsidence area. Finally, the smooth spatial and temporal character of the subsidence bowl was not fully exploited in the analysis. Although it was

possible to estimate spatial-temporal polynomials to model the behavior of local groups of benchmarks, their interpretation was rather indiscriminate.
In this paper a new analysis strategy is described for deriving land subsidence due to gas extraction from epoch networks of height difference measurements. Instead of applying an absolute deformation analysis per benchmark from connected levelling networks, a spatial-temporal trend model is estimated in a relative deformation analysis setup, if necessary followed by further analysis of the remaining subsidence signal.
In sections 2, 3 and 4 the spatial-temporal model is presented and sections 5 and 6 discuss the procedure for straightforward estimation of the subsidence from the levelling data. Two real data examples demonstrate the application of the method in sections 7 and 8.

2. Spatial-temporal subsidence modelling

Using a spatial-temporal subsidence model, the height $H_{i,t}$ of a benchmark i at time t can be written as

$$\underline{H}_{i,t} = H_{i,t_0} + z_{i,t-t_0} + \underline{\eta}_{i,t}\,, \tag{1}$$

with: H_{i,t_0} initial benchmark height before the beginning of land subsidence at t_0;
$z_{i,t-t_0}$ vertical deformation due to gas extraction since the beginning of land subsidence, that will be approximated by a spatial-temporal trend model;
$\underline{\eta}_{i,t}$ noise term accounting for the stochastic instability of the benchmark.

Model (1) states that the benchmark height behaves according to a specific deformation model, except for some individual stochastic benchmark instabilities. This so-called 'point noise' recognizes that the soft soil in The Netherlands induces some small benchmark instabilities that are not caused by the structural (in this case gas extraction driven) land subsidence that we try to model. Since the stability of a benchmark depends on its foundation and local circumstances (like variations in the ground water level), point noise is very hard to model in a general way. It is however likely to assume a random walk process for the benchmark instability: the benchmark deviation at time t_l equals the deviation at a previous time t_k, plus some white noise variation increasing with the time-lag $t_l - t_k$, i.e.

$$\underline{\eta}_l = \underline{\eta}_k + \underline{\eta}_{kl}\,, \text{ with } E\{\underline{\eta}_{kl}\} = 0\,;\; D\{\underline{\eta}_{kl}\} = (t_l - t_k)\sigma_p^2\,, \tag{2a}$$

where the point noise standard deviation σ_p is e.g. given in mm/√year. With (2a) point noise variances and covariance at two successive epochs can be written as

$$\sigma_{\eta_k}^2 = (t_k - t_1)\sigma_p^2\,,\; \sigma_{\eta_l}^2 = (t_l - t_1)\sigma_p^2\,,\; \sigma_{\eta_k\eta_l} = (t_k - t_1)\sigma_p^2\,, \qquad \text{for } t_l > t_k\,, \tag{2b}$$

with t_1 the time of the first epoch the benchmarks are measured.
Note that the point noise term $\underline{\eta}$ only accounts for the stochastic part of individual benchmark instabilities (no correlation between benchmarks). Systematic benchmark deviations from the spatial-temporal subsidence model are identified in a testing procedure that supports the estimation process (see section 5, KENSELAAR 2001 and VERHOEF ET AL. 1997).

3. A trend model for land subsidence due to gas extraction

In HOUTENBOS 2000 and KENSELAAR AND MARTENS 2000, a spatial-temporal subsidence trend model was presented for describing land subsidence due to gas extraction. According to this trend model the subsidence can be written as

$$\underline{z}_{i,t-t_0} = v(t-t_0)\exp(-\tfrac{1}{2}r_i^2) + \underline{\zeta}_{i,t-t_0} \qquad (t_0 < t < t_{\text{end}}), \tag{3}$$

with: t_0 and t_{end} times of beginning of subsidence, resp. the end of the subsidence model validity;
v subsidence velocity in the center of the subsidence bowl;
r_i standardized radius from the center of the subsidence bowl to point i;
$\underline{\zeta}_{i,t-t_0}$ noise term accounting for the stochastic discrepancies between the spatial-temporal trend model and the actual subsidence due to gas extraction.

Model (3) states that each point has a constant subsidence velocity, depending on its position in the subsidence bowl. Mainly because of the large depth (about 3000 meter) of the gas fields in The Netherlands, a smooth Gaussian-shaped bowl appears to approximate the subsidence quite well. In its simplest form the standardized radius in (3) reads

$$r_i^2 = \frac{(x_i - x_c)^2 + (y_i - y_c)^2}{r^2}, \tag{4a}$$

with: x_c and y_c coordinates of the center of the subsidence bowl;
r radius to the point of inflection of a circular subsidence bowl;

The factor ½ in (3) is introduced to accomplish that r can be interpreted as the distance to the point of inclination of the subsidence bowl. The area within $2r$ from the center then covers 95% of the volume of the subsidence bowl. In order to account for less regular shaped gas fields, an ellipsoidal subsidence pattern could act as a first refinement. Instead of (4a) we then have

$$r_i^2 = \left(\frac{(x_i - x_c)\sin\varphi + (y_i - y_c)\cos\varphi}{a}\right)^2 + \left(\frac{(x_i - x_c)\cos\varphi - (y_i - y_c)\sin\varphi}{b}\right)^2, \tag{4b}$$

with: a, b and φ long and short axes to the point of inflection and the orientation of an ellipsoidal subsidence bowl.

The adoption of linear subsidence per point in (3) is supported by long-term benchmark analysis. However, it is obvious that finally, decreasing gas reserves will violate this assumption. Therefore (3) only holds within the period of a rather constant gas pressure drop ($t_0 < t < t_{\text{end}}$). Further refinement of the temporal part of the model can easily be incorporated, e.g. with a higher order polynomial in time. Moreover, it must be emphasized that this trend model is a 'data model', with a pure geometric character: it just fits the data quite well. Although the shape of the subsidence bowl is similar to that of some simple geomechanical models, its parameters have no direct physical meaning, nor a relation with production parameters.

The stochastic noise term $\underline{\zeta}$ accounts for the imperfection of the adopted trend model (3), (4) to completely describe the real land subsidence due to gas extraction and will be denoted as 'model noise'. Zero expectation and second order stationarity can be assumed only if the trend model suits to describe the deformation without systematic biases. Even then, a model noise variance-covariance matrix is difficult to determine and will probably be case dependent. Both regional and temporal correlation of model noise terms seem plausible assumptions and several stochastic models have been proposed (HOUTENBOS 2000, LIU AND KENSELAAR 2001). If no better information is available, a simple scaled unit variance matrix can be interpreted as a necessary relaxation to make the trend model fit the data.

In the Netherlands' practice often a more complicated land subsidence pattern occurs when the subsidence of a point is induced by gas extraction from several adjacent gas fields with overlapping subsidence bowls. Instead of (3) the subsidence trend model can then be written as a superposition of elementary subsidence bowls for each gas field $\alpha = 1 \ldots nf$, i.e.

$$\underline{z}_{i,t-t_0} = \sum_{\alpha=1}^{nf} v_\alpha (t - t_{0,\alpha}) \cdot \exp(-\tfrac{1}{2} r_{i,\alpha}^2) + \underline{\zeta}_{i,t-t_0} , \tag{5}$$

where for each of the exploited gas fields the induced subsidence is approximated by a trend function (3), (4) that is expressed by 5 (circular) or 7 (ellipsoidal) parameters: the time of beginning of subsidence (t_0); the subsidence velocity in the center of the subsidence bowl (v); the coordinates of the center of the subsidence bowl (x_c , y_c); and the planar size and shape of the subsidence bowl (r in case of (4a) and a, b, φ in case of (4b)).

4. Estimation of the subsidence model from measurement data

The spatial-temporal subsidence model will be estimated from the original levelling data of the networks at all epochs. The observation equation of a levelled spatial height difference in epoch k reads

$$\underline{h}_{ij,k} = -H_{i,t_k} + H_{j,t_k} + \underline{\varepsilon}_{ij,k} , \tag{6}$$

where the stochastic noise term $\underline{\varepsilon}$ accounts for the levelling measurement inaccuracy, further denoted as 'measurement noise'. For the stochastic model of levelling observations usually no correlation is assumed, while the variances increase with the length of the levelling line, i.e.

$$\sigma_{\varepsilon_{ij,k}}^2 = \sigma_{l_k}^2 l_{ij} , \tag{7}$$

where the measurement noise standard deviation σ_l is given in mm/√km and can be specified per epoch (k). For accuracy levelling values between 0.5 and 1.0 mm/√km are usual.
Replacing the heights in (6) by the spatial-temporal subsidence model (1), using a trend model (3) or (5), results in

$$\underline{h}_{ij,k} = -H_{i,t_0} + H_{j,t_0} - z_{i,t_k-t_0} + z_{j,t_k-t_0} + \underline{e}_{ij,k} , \tag{8}$$

with the stochastic noise term $\underline{e}$ as the lump sum of measurement noise in (6), point noise in (1) and model noise in (3):

$$\underline{e}_{ij,k} = \underline{\varepsilon}_{ij,k} - \underline{\eta}_{i,k} + \underline{\eta}_{j,k} - \underline{\zeta}_{i,t_k-t_0} + \underline{\zeta}_{j,t_k-t_0} . \tag{9}$$

The unknowns in observation equation (8) are the initial heights of two benchmarks and the trend model parameters. After linearization of the trend function, the linearized model of observation equations for a levelling network at a single epoch k can be written as

$$\Delta\underline{h}_k = W_k \begin{pmatrix} P_k & Z_k \end{pmatrix} \begin{pmatrix} \Delta H_0 \\ \Delta p \end{pmatrix} + \underline{e}_{h_k} \; ; \quad Q_{h_k} = Q_{l_k} + W_k (Q_{p_k} + Q_{m_k}) W_k^T , \tag{10}$$

with: Δh_k vector of m_k linearized levelled height differences in the levelling network at epoch k;

W_k matrix relating the levelled height differences and benchmark heights at epoch k (the levelling network design matrix);
P_k permutation matrix selecting the nb_k benchmarks occupied at epoch k from the complete set of nb benchmarks;
Z_k $nb_k \times np$ coefficient matrix containing the partial derivatives of equations (3) or (5), and (4), to the unknown parameters of the trend model;
ΔH_0 vector of nb linearized initial benchmark heights;
Δp vector of np linearized trend model parameters describing the subsidence bowl;
e_{h_k} vector of m_k unknown noise terms;
Q_{l_k} variance matrix for the m_k measurement noise terms in the network at epoch k;
Q_{p_k} variance-covariance matrix for the nb_k point noise terms of the benchmarks at epoch k;
Q_{m_k} variance-covariance matrix for the nb_k model noise terms at epoch k.

The levelling variance matrix Q_l is a diagonal matrix, computed with (7). The point noise variance-covariance matrix Q_p has zero-rows and -columns for the first epoch, zero covariance between benchmarks, but non-zero covariance between the heights of a benchmark at different epochs, according to (2b). The model noise variance-covariance matrix Q_m contains zeros for all epochs before the beginning of subsidence, since the adopted trend model is perfect if there is no subsidence yet. Before gas extraction, all discrepancies should be explainable by levelling noise and point noise only.

The subsidence model is estimated from the data at all available epochs. The integrated model contains Σm_k observations and $nb+np$ unknowns, with nb the number of benchmarks and np the number of parameters of the trend model. As an example, we give the multi-epoch model for four epochs of data, with the first one before the beginning of subsidence:

$$\begin{pmatrix} \Delta\underline{h}_1 \\ \Delta\underline{h}_2 \\ \Delta\underline{h}_3 \\ \Delta\underline{h}_4 \end{pmatrix} = \begin{pmatrix} W_1 & & & \\ & W_2 & & \\ & & W_3 & \\ & & & W_4 \end{pmatrix} \begin{pmatrix} P_1 & O \\ P_2 & Z_2 \\ P_3 & Z_3 \\ P_4 & Z_4 \end{pmatrix} \begin{pmatrix} \Delta H_0 \\ \Delta p \end{pmatrix} + \begin{pmatrix} \underline{e}_{h_1} \\ \underline{e}_{h_2} \\ \underline{e}_{h_3} \\ \underline{e}_{h_4} \end{pmatrix}. \qquad (11)$$

All (multiples of) 5 or 7 parameters of the trend model can be determined if levelling observations at three or more epochs are available, with at least one epoch before the beginning of subsidence. As an alternative one could constrain one or more parameters, or add them as pseudo observations if valid a priori information is available. For instance, information about the time of beginning of subsidence can be obtained from gas production data.
Since (initial) heights are determined from height differences, the model is rank defect. In order to solve this problem is sufficient to constrain the initial height of one benchmark at an a priori value. This choice influences the resulting initial heights by a height translation, but not the determined subsidence itself. The base-point benchmark does not need to be stable or observed at all epochs.

5. Trend-signal analysis

The best fitting subsidence model is determined in a stepwise procedure of least-squares adjustment, statistical hypothesis testing and adaptation of both the data and model. In each step the actual model and data – the so-called null hypothesis model – are tested against a large number of alternative hypotheses, each suggesting a specific model adaptation or possible error(s) in the data. Presently the following types of alternative hypotheses are considered:

- Observation tests, for an individual error in the levelling data (datasnooping);

- Identification tests, for deviating behavior of a specific benchmark at one specific epoch;
- Point tests, for a general deviating behavior of a specific benchmark;
- ALB tests, assuming autonomous linear behavior (ALB) of a specific benchmark, i.e. the benchmark has a constant velocity, but significantly different from the trend model;
- Epoch tests, indicating the data of a complete epoch deviates from the model, without further specification;
- Overall model test, indicating that model and data just don't match, without further specification.

As long as the null hypothesis is rejected, the most significant error or model adaptation is suggested by the largest test quotient (quotient of test quantity and critical value). Adaptations could consist of mutations in the data, addition of unknown parameters, like ALB velocities for specific benchmarks, or adaptations in the stochastic model, e.g. increasing the model noise variance. The adapted model acts as new null hypothesis in the next step of estimation and testing, until all tests are accepted. This testing procedure is treated in more detail in KENSELAAR 2001.

Least-squares estimates for the parameters of the best fitting subsidence bowl are obtained from the (accepted) model, as well as their precision. Since this precision is based on application of the law of propagation of (co)variances to the complete covariance matrix Q_h, it includes levelling measurement noise, point noise, as well as the necessary model noise (co)variance to make the model accepted by the testing. With the spatial-temporal model, the subsidence can be computed for any point within the subsidence area at any time since t_0. It must however be emphasized that one should be careful using the model for prediction of land subsidence beyond the last epoch. Since the model simply assumes a constant velocity and does not contain any production parameters (like pressure drop and remaining gas reserves), computation of future subsidence is e.g. only valid to explore the best moment for the next epoch of levelling survey.

The subsidence due to gas extraction is defined in (3) as the sum of a trend model plus model noise: the remaining discrepancies between actual gas-driven subsidence and trend model. Since the trend model can be considered a good global approximation, further detail can be revealed from that part of the least-squares residuals $\hat{e}_h$ that can be assigned to model noise. Least-squares estimators of the model noise terms can be computed per epoch as

$$\underline{\hat{\zeta}}_k = Q_{m_k} W_k^T (Q_h^{-1} \underline{\hat{e}}_h)_k , \tag{12}$$

with $(Q_h^{-1} \underline{\hat{e}}_h)_k$ a vector with m_k elements of the matrix-vector product $Q_h^{-1} \underline{\hat{e}}_h$, related to the observables of epoch k.
Estimation of the model noise terms recovers the 'signal': the remaining subsidence after subtraction of the trend from the measurement data. With (12) the signal can be separated from the measurement noise and individual benchmark point noise in the least-squares residuals. Visualization of this signal could e.g. reveal local area deviations from the global trend. The signal can also be computed at other arbitrary positions and times if the model noise variance-covariance matrix assumes spatial, resp. time correlation. This approach will be demonstrated in sections 7 and 8. Note that computation of the signal with (12) is highly dependent on the a priori model noise covariance matrix Q_m. Since this matrix is in general not well known, careful investigation of the computed signal and further research is necessary, e.g. by empirical determination of a model noise covariance function from the data.

6. Discussion

Figure 1 summarizes the stepwise subsidence analysis procedure, as described in brief in section 1, versus the new approach, as presented above.
Maybe the main advantage of this integrated approach is not the use of a specific subsidence trend model, nor the introduction of spatial-temporal subsidence modelling. For the practice of

subsidence monitoring surveying, it is the approach of relative deformation analysis from levelling observations that supplies a major advantage over absolute deformation analysis from benchmark heights (which requires the connection of the epoch networks to stable reference points). Especially in the Netherlands this implies extension of the levelling networks far outside the subsidence area. And then still, it is hard to find undoubtedly stable reference points for the whole monitoring period.

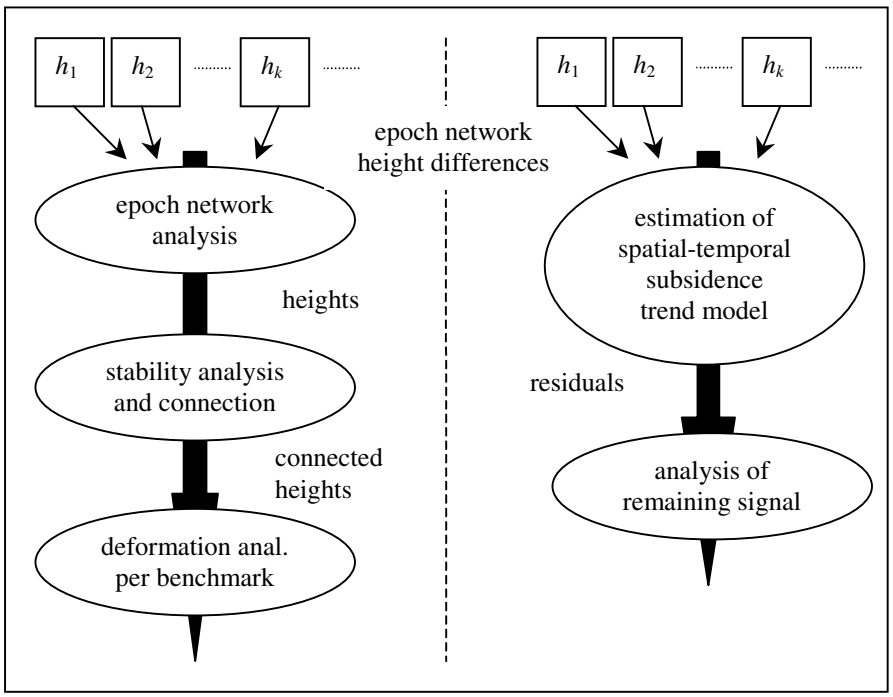

Figure 1: 3-step absolute subsidence analysis procedure (left) versus integrated relative subsidence analysis using a spatial-temporal subsidence model (right).

Instead of recovering a spatial pattern in the estimated subsidence per benchmark, direct estimation of a spatial-temporal model could be beneficial, as long as a reasonable model can be specified. It allows a clear spatial interpretation of the phenomenon and supports the understanding of geophysical models for the prediction of land subsidence. Furthermore, integration of different measurement methods becomes much easier. For example, levelled spatial height differences and GPS derived temporal height differences need not be measured at combined benchmarks, since the spatial-temporal model itself connects both data sources.
Also a more efficient design of the levelling networks might be possible. Not only because the connection to stable reference points can be omitted, but also since redundancy of the epoch networks is no longer a prerequisite. Redundancy follows from the total number of levelling observations in all epochs, minus the number of benchmarks and trend model parameters. As long as the multi-epoch network is computable, sparse epoch networks like profiles may be allowed. Optimal design of the measurement strategy in time, space and topology, can be obtained from a-priori studies for precision and reliability (KENSELAAR AND MARTENS 2000).

A complex physical phenomenon like land subsidence due to gas extraction can probably never be modelled exactly. Instead of efforts to improve the modelling by raising the complexity of the model and the number of parameters, e.g. using high-order spatial-temporal polynomials, it was chosen to use trend-signal analysis. A simple trend model with a clear geometric interpretation acts as a reasonably good first approximation (in the next two sections we will demonstrate how good). It is known to be an imperfect description of the real but unknown gas extraction induced subsidence, and the remaining discrepancies (the signal) are modelled in a statistical way.
Investigation of the signal is of importance since the extent of spatial correlation is revealing whether the vertical movements have a shallow cause or a cause at greater depth. If the null

hypothesis is being accepted by adding model noise in the stochastic model, based on a covariance function with a large spatial correlation length, one is confident that the cause is at considerable depth. The visualized signal should then reveal a strong regional coherence: neighboring benchmarks show similar deviations from the trend model. However, if the model only fits with a very small spatial correlation length, then little or no spatial coherent behavior is present in the benchmarks. This is likely to result from more shallow causes than gas extraction and should be accounted for as point noise.
With the gradual depletion of the reservoir as a driving force, also time correlation is likely to show up in the signal. The causal separation of subsidence can be of importance for a fair allocation of damage compensation costs to the oil company.

7. Example: an isolated gas and oil field

In '79, '84, '89, '91, '92, '95 and '99 spirit levelling surveys were carried out over a field in The Netherlands, where the depletion of the gas and oil reservoir started in 1984. In total this yielded 634 observations between 171 benchmarks, resulting in a redundancy of 456. Initially, the stochastic model consisted of measurement noise with a standard deviation of 0.7 mm/√km, and point noise with a standard deviation of 0.6 mm/√year, according to (2). In the estimation and testing procedure, successive model adaptations were undertaken based on evaluating the alternative hypothesis with the largest rejected test quotient. Still, a number of test quotients (slightly) exceeded the critical value. Finally, the null hypothesis was accepted with the extension of the stochastic model with model noise according to a covariance function

$$\sigma_{\zeta_{i,k},\zeta_{j,k}} = \sigma_m^2 (t_k - t_1) e^{-\left(\frac{l_{ij}}{L}\right)^2}, \qquad (13)$$

which specifies the model noise covariance between the heights of benchmarks i and j at a distance l_{ij} at time t_k, t_1 is the time of the first epoch and L is the correlation length. In this case L was taken 1 km and σ_m = 2 mm/√year. Since the subsidence trend model velocity was estimated at an insignificant 0.0001 mm/year, the only way to obtain information about subsidence is by mapping the signal. The signal is computed at a grid of 50 m and can be found in figure 2. The relative short correlation length could indicate that the point noise was too low. On the other hand, if any coherence is present in the signal, it will be shown as well with a short correlation length. Confrontation of figure 2 with production information revealed that water injection is taken place in three wells in the southeast part of the reservoir, which could possibly result in coherent land rise rather than subsidence.

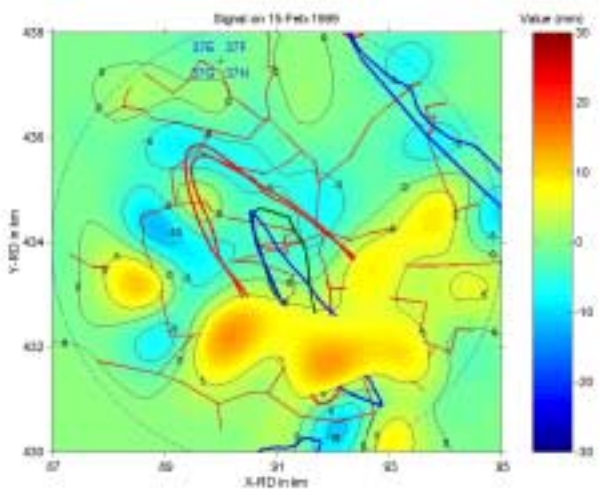

Figure 2: Spatial signal, with the levelling trajectories in red. The outlines of the oil field, gas field and acquifer are drawn in red, green and blue respectively.

8. Example: complicated subsidence pattern

The second data set examined in this paper is much more extensive and complex than the previous one. This so-called Tietjerk-Suawoude data set covers two adjacent gas fields (centers 6.5 km apart) with overlapping subsidence bowls and a third gas field in the southeast. This necessitated the use of a superposition trend model (5). The data set contains 11 epochs between 1970 and 1999. Most of the epoch networks are quite dense and cover a larger area than the subsidence bowl. After area selection and data reduction the data set still contains 1537 height differences and 262 benchmarks. The estimation and testing procedure was started with measurement noise standard deviations between 0.6 and 0.9 mm/√km per epoch and a point noise standard deviation of 0.6 mm/√year. Initially zero model noise was assumed. After some model adaptations the model was still rejected. Especially large test quotients were identified for benchmark ALB-velocity tests in the south.
Since the null hypothesis, consisting of three bowls, was not accepted, model noise was accounted for in the stochastic model conform (13), with a correlation length of 3 km and a standard deviation σ_m = 0.5 mm/√year. Mapping the signal revealed coherent subsidence in the south, dominating other movements as the apparent land rise in the north. This can be seen in figure 3 (left). The sum of signal and the estimated model is shown in figure 3 (right). In table 1 the estimated parameters of the three bowls are summarized.
In the studied area another cause for subsidence appears to be present, caused by another oil company. Finally, an accepted model was achieved via careful selection of benchmarks that were not influenced by the subsidence in the south. The trend model was then accepted without accounting for any model noise. The precision of the estimated subsidence can then be computed by applying the propagation law of variances to the precision of the estimated trend model parameters. Resulting subsidence and precision are presented in figure 4. This precision is steering the design and frequency of successive surveys.

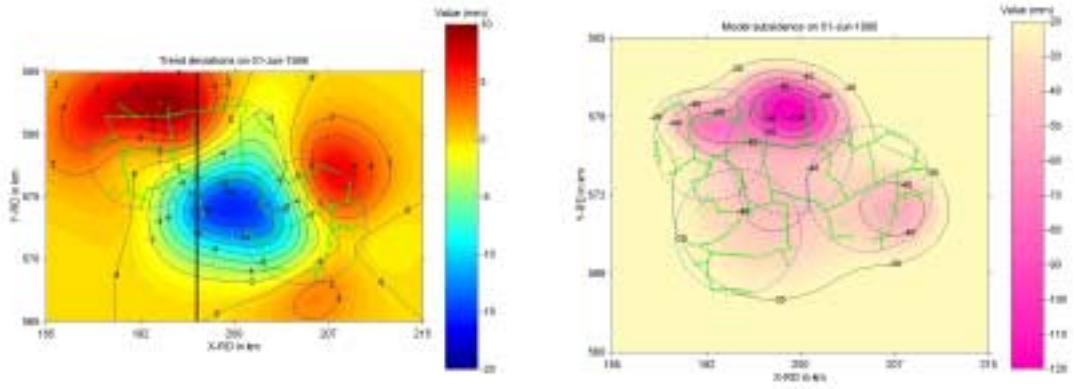

Figure 3: Signal revealing coherent subsidence (left), and the sum of trend model and signal (right). In green the levelling trajectories.

Parameter	East bowl	West bowl	South East bowl
Subsidence velocity (mm/year)	-5.9	-8.2	-3.1
Beginning of subsidence	March 16, 1977	January 30, 1992	March 29, 1984
X-position center of bowl (m)	199077	192774	207436
Y-position center of bowl (m)	578999	578059	571348
Half long axis subsidence bowl (m)	2382	2496	3096
Half short axis subsidence bowl (m)	1639	1493	
Orientation of subsidence ellipse (gon)	103.1	115.0	

Table 1: Estimated parameters of the three bowls. Note the shape of the southeast bowl is a circle.

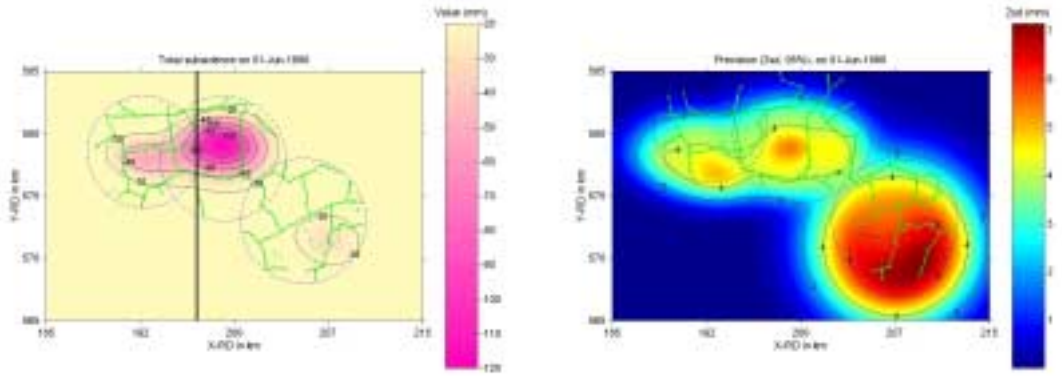

Figure 4: The final estimation of three bowls after careful selection of levelling trajectories (left), and the precision of the estimated subsidence (right).

9. Concluding remarks

Research is still going on. Further research topics include the estimation of empirical variance-covariance functions for point noise and model noise; a better understanding of the relation with subsidence prediction models from geomechanics and production data; refinements of the trend model applied; and integration with other measurement techniques, like GPS and InSAR.

References

Barends, F.B.J., F.J.J. Brouwer, F.H. Schröder (eds.) (1995). *Land Subsidence, proceedings of the IAHS Fifth International Symposium On Land Subsidence (FISOLS)*, The Hague, Balkema, Rotterdam (ISBN 0-947571-74-4).

Heus, H.M. de, M.H.F. Martens, H.M.E. Verhoef (1994). Stability-analysis as part of the strategy for the analysis of the Groningen gasfield levellings. In: *Proceedings of the Perlmutter Workshop on Dynamic Deformation Models*, Haifa, pp 259-272.

Heus, H.M. de, P. Joosten, M.H.F. Martens, H.M.E. Verhoef (1995). Strategy for the analysis of the Groningen gas field levellings - an overview. In: *Land Subsidence, proceedings of the IAHS Fifth International Symposium On Land Subsidence (FISOLS)*, the Hague (ISBN 0-947571-74-4), pp.301-311.

Houtenbos, A.P.E.M. (2000). The quantification of subsidence due to gas-extraction in the Netherlands. In: *Land Subsidence, proceedings of the IAHS Sixth International Symposium On Land Subsidence (SISOLS)*, Italy (ISBN 88-87222-06-1), pp. 177-189.

Kenselaar, F., M.H.F. Martens (2000). Spatial-temporal modelling of land subsidence due to gas extraction. In: *Land Subsidence, proceedings of the IAHS Sixth International Symposium On Land Subsidence (SISOLS)*, Italy (ISBN 88-87222-06-1), pp. 383-396.

Kenselaar, F. (2001). A testing procedure for subsidence analysis. In: *Proceedings of the 10th FIG International Symposium on Deformation Measurements*, Orange, California, March 19-22.

Liu, Q.W. (2001). Considering the model noise when modelling land subsidence bowls due to gas extraction in the Netherlands. Submitted to *Zeitschrift für Vermessungswesen*.

Verhoef, H.M.E. and H.M. de Heus (1995). On the estimation of polynomial breakpoints in the subsidence of the Groningen gas field. *Survey Review*, Vol.33, no.2, pp.17-31.

Verhoef, H.M.E., P. Joosten and H.M. de Heus (1997). Subsidence analysis in the Netherlands Groningen gas field and the detection of (locally) unfitting points. In: *Proceedings of the IAG regional symposium on deformation and crustal movement investigations using geodetic techniques*, Hungary, pp. 159-166.